Phys. Status Solidi A **207**, No. 8, 1880–1886 (2010) / **DOI** 10.1002/pssa.200925286

physica status solidi a
www.pss-a.com
applications and materials science

Synthesis of band gap engineered $Pb_xCd_{1-x}Se$ thin films: A study on their optical, electrical, structural and localized mechanical properties

Nillohit Mukherjee[1], Gobinda Gopal Khan[2], Arijit Sinha[2], and Anup Mondal*[,1]

[1] Department of Chemistry, Bengal Engineering and Science University, Shibpur, Botanic Garden, Howrah 711 103, West Bengal, India
[2] School of Materials Science and Engineering, Bengal Engineering and Science University, Shibpur, Botanic Garden, Howrah 711 103, West Bengal, India

Received 3 June 2009, revised 11 January 2010, accepted 13 January 2010
Published online 1 March 2010

Keywords optical properties, electrical properties, thin film ternary compound, band-gap engineering, mechanical properties

* Corresponding author: e-mail anupmondal2000@yahoo.co.in, Phone: +913326684561, Fax: +913326682916

In this work, we report a novel electrochemical technique to prepare band gap engineered IV–II–VI type ternary solid solution system of $Pb_xCd_{1-x}Se$. This technologically important material is prepared using this method for the first time. We have used a self sufficient modified electrochemical cell made up of Pb anode and a transparent conducting oxide (TCO) coated glass cathode, containing $Pb(CH_3COO)_2$, $Cd(CH_3COO)_2$, H_2SeO_3 and Na_2EDTA solutions with proper concentrations as the working electrolyte. X-ray diffraction (XRD) pattern analysis confirms the formation of highly crystalline $Pb_xCd_{1-x}Se$, whereas, scanning electron micrograms (SEM) reveals a uniform deposition with compact surface morphology. This ternary system showed band gap energy (E_g) of about 1.4 eV, which is in between CdSe (1.77 eV) and PbSe (0.3 eV) and reasonably good for solar energy absorption. Good rectifying behaviour of the TCO/ $Pb_xCd_{1-x}Se$ hetero-junction was established from the current–voltage measurements, which indicate the p-type conduction nature of the deposited ternary compound. Mechanical properties of such thin films were measured by nano-indentation.

1 Introduction Recently, solid solutions with semiconducting properties are of interest due to their potential applications in the cutting edge science and technology. Some well-studied isoelectronic alloys or ternary compounds are $Pb_{1-x}Sn_xTe$, $Pb_{1-x}Sn_xSe$ and $PbS_{1-x}Se_x$. These are the series of IV–VI compounds and find applications as thermoelectric materials [1], mid-infrared lasers [2], diode lasers [3–5], infrared detectors [6], mechanical alloys [7], etc. In this regard, cadmium-lead-chalcogenide (II-IV-VI system) [8] and cadmium-zinc-chalcogenide (II-II-VI system) [9] ternary compounds have attracted the attention of workers for their similar interesting properties. The preparative methods for these compounds are not well established till date, and here an easy electrochemical technique to deposit band gap engineered $Pb_xCd_{1-x}Se$ thin films is reported for the first time.

It begins with the idea that, the E_g of n-CdSe (~1.76 eV at room temperature for the bulk system) is not good enough for a window layer in solid state solar cells. Again, p-PbSe has a too low E_g (~0.3 eV, room temperature, bulk system) to be used as an absorber material. An easy electrochemical technique has been reported earlier for the preparation of PbX (X = S, Se and Te) [10] and CdSe [11]. However, an appropriate combination of the working electrolytes for the deposition of the two materials can lead to form a ternary system, $Pb_xCd_{1-x}Se$, which can make the material to have an optimum E_g of about 1.4–1.5 eV, which would be very close to an ideal absorber layer. The electrochemical cell we have used for this purpose contained aqueous solutions of $Pb(CH_3COO)_2$, $Cd(CH_3COO)_2$ and H_2SeO_3 in appropriate concentrations. Na_2EDTA solution was added as a complexing agent for regulated deposition. The TCO substrate was used as the cathode, while a 99.9% pure metallic Pb strip was used as a self-decaying anode. When the two electrodes were short circuited externally, uniform and highly adherent thin films of $Pb_xCd_{1-x}Se$ were deposited on the TCO surface. The beauty of this process is that it dose not require any

external energy for deposition, the overall cell potential serves the need. Optical, morphological, compositional, mechanical and structural characterizations of the films were carried out by UV–VIS, SEM, EDX, Nano-indentation and XRD techniques. Electrical properties were also measured to establish its probable application as a solar cell material. From UV–VIS spectrum, the onset of a sharp increase in absorption was evident around ~900 nm; which corresponds to an E_g of about 1.4 eV. SEM image indicates a compact surface morphology. Mechanical properties of such films have been studied and reported for the first time. The hardness values, H_v (Vickers) and the instrumented elastic modulus values E_{IT} (GPa), revealed that both the hardness and the modulus of the coated surface under 40 mN load was high enough to produce better resistance towards the deformation caused under thermal stresses while exposed to the nature for practical applications.

2 Experimental

2.1 Deposition procedure To start with, the substrates were cleaned with detergent and then dipped into concentrated chromic acid solution for about 30 min and washed thoroughly with distilled water to remove any adhering impurities. They were then boiled in methanol and after drying were degreased in a vapor of trichloroethelene.

Recently, PbSe thin films on TCO coated glass substrates were deposited by us [10] using a self sufficient galvanic cell containing aqueous solutions of $Pb(CH_3COO)_2$, Na_2EDTA and SeO_2 at pH 3, whereas, Murali et al. [11] in 1990 reported the deposition of CdSe using the same technique. Here, a properly cleaned TCO glass substrate and a Pb strip were dipped into a solution containing 10 ml 0.1 M $Pb(CH_3COO)_2$, 5 ml 0.1 M $Cd(CH_3COO)_2$ and 10 ml 0.1 M aqueous SeO_2 solutions (Bath B). 10–15 ml 0.1 M aqueous Na_2EDTA solution was also added to the solution before the addition of selenous acid, as a complexing agent for regulated deposition. The overall volume of the solution was made up to 100 ml. The schematic of the process is reported in Ref. [10]. We have varied the amount of $Cd(CH_3COO)_2$ from 3 ml (Bath A) to 8 ml (Bath C), keeping the amount of $Pb(CH_3COO)_2$ fixed, and found that films with excellent optical, electrical and structural properties were resulted when 5 ml $Cd(CH_3COO)_2$ was taken (Bath B). The Pb strip and the TCO glass substrate were short-circuited externally through a copper wire. The Pb strip served as a self-decaying anode and the TCO glass substrate as the cathode. The pH of the solution was kept at 3, which was found to be optimum for $Pb_xCd_{1-x}Se$ film deposition. The deposition was carried out for 60 min (where the saturation in thickness was obtained) at temperature 70 – 75 °C. The solutions were stirred continuously during deposition.

2.2 Characterizations XRD pattern of the film was taken by a SEIFERT P3000 Parallel Beam X-ray Diffractometer with Cu K_α ($\lambda = 1.540598$ Å) X-radiation and θ–2θ scanning mechanism. The SEM images of the deposited films were taken by a HITACHI S 3400 N scanning electron microscope fitted with HORIBA 7021-H EDX probe. Optical measurements were carried out using a JASCO V 530 UV–VIS spectrophotometer. The electrical (current–voltage) measurements were performed using a KEITHLEY SCS 4200 Semiconductor Characterization System and the mechanical properties were studied using CSM Instruments: NHTX 50-0019 nanohardness tester.

3 Results and discussion

3.1 The chemistry When SeO_2 is dissolved in water, it easily produces selenous acid (H_2SeO_3), which dissociates in solution to $2H^+$ and SeO_3^{2-} ions. The Pb^{2+} and Cd^{2+} ions were first complexed with the addition of Na_2EDTA solution, followed by the addition of H_2SeO_3 solution, to prevent any precipitation of $PbSeO_3$ and $CdSeO_3$. Glacial CH_3COOH was added to the solution to prevent hydrolysis of the lead and cadmium salt and also to maintain the optimum pH (~3) of the solution for deposition. The controlled dissociation of the electrolytes $Pb(CH_3COO)_2$ and $Cd(CH_3COO)_2$ in solution is also achieved by the common ion effect of CH_3COO^- ion produced by CH_3COOH. When the Pb strip and the TCO substrate were dipped into the solution and short circuited externally by a copper wire, elemental Pb from the anode dissolves into the solution forming Pb^{2+} ions, $Pb \rightarrow Pb^{2+} + 2e$ ($E^0 = +0.126$ V). The electrons that were released moved through the externally short-circuited path to the TCO electrode and carry out the required cathodic reduction. The Pb^{2+} and Cd^{2+} ions present in the solution are attracted by the TCO cathode and thereby get discharged on the cathode surface simultaneously, by taking up electrons. We propose the following overall cathode reactions to take place for this system:

$$Pb^{2+} + Cd^{2+} + SeO_3^{2-} + 6H^+ + 8e \rightarrow Pb_xCd_{1-x}Se + 3H_2O (0 < x < 1)$$

Since, the amount of Cd^{2+} ions is lesser than that of Pb^{2+} ions in the solution, and the reduction potential of Cd^{2+} ion is more negative than that of Pb^{2+} ion, it is obvious that lesser amount of cadmium will contribute to the matrix of the deposited film leading to the composition of the film as $Pb_xCd_{1-x}Se$.

3.2 Film growth kinetics In order to study the growth rate of the films obtained from the three baths, the thickness of the films was measured gravimetrically, time to time, using AB54S Mettler balance (fourth decimal). The thickness of the films was plotted as a function of time, from which an idea on the film growth rate was obtained. It has been found that the saturation thickness at 75 °C was achieved nearly after 60 min with an almost same growth rate of 0.03 μm/min, for the three baths. Since, there was no continuous supply of SeO_3^{2-} ions solution, the formation of films on cathode surface stops after a certain time, when the

SeO_3^{2-} ions get exhausted, as the reduction potential of $SeO_3^{2-} + 6H^+ + 4e \rightarrow Se + 3H_2O$ ($E^\circ = +0.74$ V) system mainly provides the driving force for the overall cathode reaction.

3.3 Variation of cathode current density The variation of cathode current density (I) with respect to time (t) for the deposition process from all three baths was measured against a standard resistance of 0.8 Ω. The current densities were calculated from the potential values obtained after short-circuiting the two electrodes. A sharp fall in I was found to occur during the first hundred seconds. The steady cathode current density was found to reach nearly after 200 s and it was ~0.9 mA/cm^2. The steady overall cell potential was calculated to be around 0.72 V, high enough as the driving force to carry out the desired reactions. The values were nearly the same for the three different baths; since the driving force for all the systems was mainly the reduction of SeO_3^{2-} to Se.

3.4 X-ray diffraction study The XRD pattern of the films deposited at 75 °C from Bath A, Bath B and Bath C are shown in Fig. 1a–c, respectively. It is evident from Fig. 1a that the films obtained from Bath A consists mainly of PbSe (JCPDS ID 06-0354) with the beginning of the formation of $Pb_xCd_{1-x}Se$. On the other hand, the films from Bath C were found to be composed mainly of CdSe (JCPDS ID 08-0459) with some traces of $Pb_xCd_{1-x}Se$ and PbSe, whereas, films with our desired composition, *i.e.* $Pb_xCd_{1-x}Se$ were obtained only from Bath B, where we find no traces of other materials like PbSe or CdSe as impurities. Since the reduction potential of Cd^{2+} ion is more negative than that of Pb^{2+} ion, and the reaction is carried out under a fixed value of potential, controlling the amount/concentration of Pb^{2+} and Cd^{2+} ions in the working solution is crucial in order to obtain the films with desired composition by the competitive migration and reduction of the ions at the TCO cathode. Here we see that the electrolytic combination of Bath B is appropriate for the deposition of $Pb_xCd_{1-x}Se$ ternary solid solution system. Figure 1b reveals the presence of two new peaks at $2\theta = 43.664$ and 65.653 degrees. These two diffraction peaks do not match with any diffraction plane of CdSe (JCPDS ref. 08-0459) and/or PbSe (JCPDS ref. 06-0354); hence, we propose that, the diffractions that occur at these angles are from the newly deposited ternary solid solution compound $Pb_xCd_{1-x}Se$. Absence of any diffraction peak corresponding to CdSe and/or PbSe confirms the fact that there is no deposition of free CdSe or PbSe along with the $Pb_xCd_{1-x}Se$ film. The peaks marked '*' in the figure are for the SnO_2 of the TCO substrate (JCPDS ref. 21-1250). The crystallite sizes of the deposited films were calculated from the most intense XRD peak for each case, using Scherrer equation; $D = 0.9\,\lambda/(\beta\cos\theta)$, where, λ is the wavelength of the X-radiation (1.54056 Å), β is the value of FWHM of the peak of highest intensity and θ is the diffraction angle. The average crystallite size was calculated to be around 200 and 100 nm for the films obtained from Bath A and Bath C, whereas, for the $Pb_xCd_{1-x}Se$ film (from Bath B), it was around 100 nm.

3.5 Scanning electron micrograph and energy dispersive X-ray spectroscopy analysis Figure 2a–c are the representative SEM images of the films obtained from the Baths A, B and C, respectively. The thicknesses of the films chosen for SEM measurements were in the same range. Good coverage of the TCO surface by the uniformly deposited films from the three baths is evident from the images. The shape of the grains of this newly deposited material (from Bath B) is found to be cubic with the average grain size of about 250 nm, whereas, the shape of the grains of the films with predominantly PbSe (from Bath A) and CdSe (from Bath C) in it were found be nearly spherical and like coffee beans, respectively. The average grain sizes of the films obtained from Bath A and Bath C were 500 nm and 250 nm, respectively. From XRD measurement it was observed that the crystallite sizes were about 200, 100 and 100 nm, respectively for the films obtained from Baths A, B and C. It is a well-established fact that small crystallites coalesced together to from grains with large size, which is seen by SEM.

The compositional details of the film were read out from the representative EDX spectrum of the ternary material

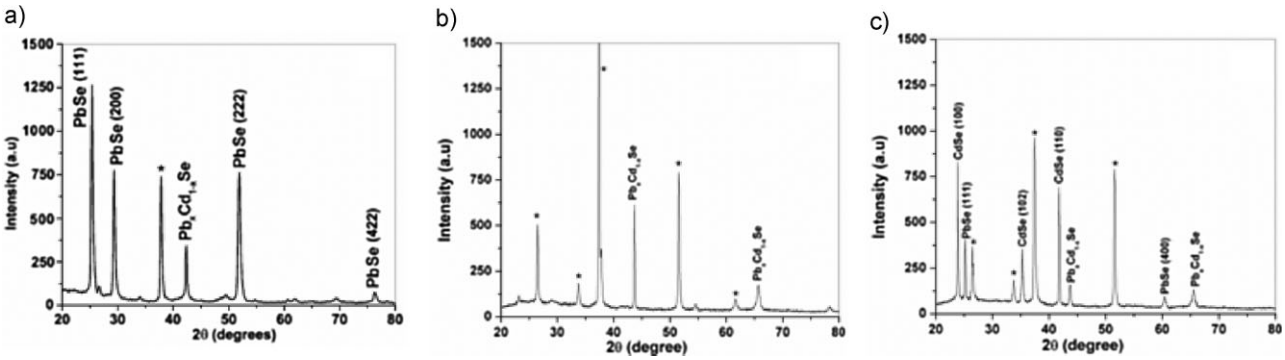

Figure 1 X-ray diffraction patterns for the films deposited from (a) Bath A, (b) Bath B, and (c) Bath C. The '*' marked peaks are for the SnO_2 of the TCO substrate.

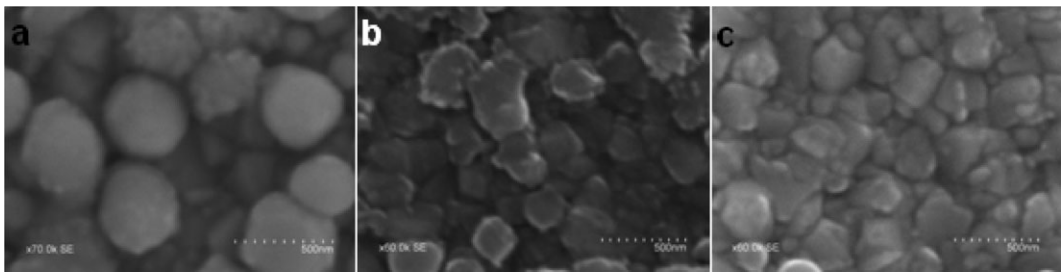

Figure 2 SEM images of the films deposited from (a) Bath A, (b) Bath B, and (c) Bath C on TCO-coated glass substrates.

$Pb_xCd_{1-x}Se$, which indicates the presence of the elements Se, Pb and Cd. The result of quantitative EDX analyses shows that the ratio of atomic percentage of Se, Pb and Cd is 51:34:15. From this measurement, we propose the approximate stoichiometry of the $Pb_xCd_{1-x}Se$ film to be $Pb_{0.7}Cd_{0.3}Se$. However, the films are likely to be slightly selenium reach, leading to the p-type conductivity of the deposited material. The proposed stoichiometry (from EDX analyses) for the other two types of films obtained from the Baths A and C are $Pb_{0.8}Cd_{0.2}Se$ and $Pb_{0.2}Cd_{0.8}Se$, respectively. These values indicate that, predominantly PbSe and CdSe were formed from the Baths A and C, which also support the outcome of XRD analyses.

3.6 Optical (UV–VIS) studies The UV–VIS spectral analysis of the films from Bath B was carried out and a sharp rise in absorbance was observed at a wavelength near 900 nm (Fig. 3, curve b), which corresponds to the band gap energy (1.4 eV) of the deposited $Pb_xCd_{1-x}Se$ film. A thorough scan from 4 000 nm was also performed to detect any presence of free PbSe, but no such absorption edge was observed (the result is not shown here) for such films. The sharp increase in the absorption spectra indicates good crystalline nature of the films. The band gap energy (1.4 eV) is close to the ideal value (1.4–1.5 eV) for application as a photovoltaic material [12].

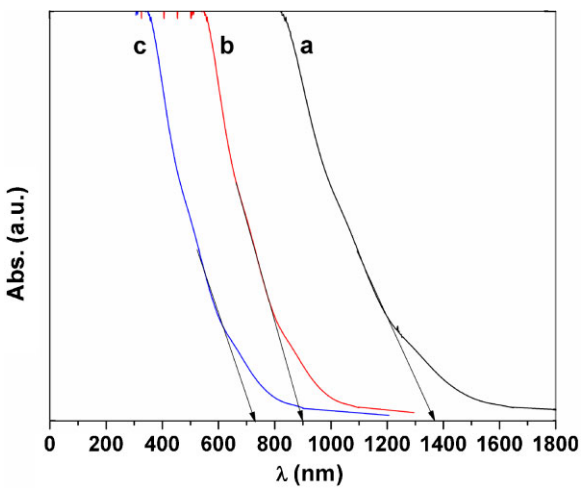

Figure 3 (online colour at: www.pss-a.com) UV–VIS absorption spectra of the films deposited from (a) Bath A, (b) Bath B, and (c) Bath C.

From XRD pattern analyses and EDX measurements it is evident that the films obtained from Bath A contains mainly PbSe and that from Bath C contains mainly CdSe, which also has influence on the respective optical data. From curve a of Fig. 3, which is for the films obtained from Bath A, we can locate the sharp rise in the absorption spectrum close from 1 400 nm (corresponding to $E_g = 0.9$ eV), which is moving towards the E_g of PbSe (~0.3 eV), but is not exactly the same, since it has some $Pb_xCd_{1-x}Se$ ternary compound mixed with it, the value is to some extent higher. On the other hand, as the films obtained from Bath C contains mainly CdSe and traces of PbSe and $Pb_xCd_{1-x}Se$ ternary systems, the rise in the optical absorption curve starts from around 730 nm (curve 'c'), which corresponds to the $E_g = 1.7$ eV and close to the typical value for CdSe ($E_g = 1.76$ eV). The observations relating bath composition, film stoichiometry and band gap energy are summarized in Table 1.

3.7 Studies on mechanical properties The sustainability/stability of the thin films at adverse conditions depends on its mechanical properties. The nanoindentation technique is used for the estimation of mechanical properties of the thin film materials [13]. The mechanical properties of $Pb_xCd_{1-x}Se$ thin films deposited on TCO glass has been reported here for the first time, by nanoindentation measurements. In this technique, a load is applied to a triangular pyramidal shaped diamond indenter tip(Berkovich) which penetrates the surface of the films being tested. One of the impressions of the indenter is captured by the inbuilt atomic force microscope (AFM) of the instrument and is shown in Fig. 4. The selected scan area was 14 μm × 14 μm. Analyses of the load vs. depth of penetration plots yielded the elastic modulus (E_{IT}) [14] and hardness (H_{IT}) [14], following the inbuilt Oliver & Pharr algorithm as

$$E_{IT} = (1 - \nu_s^2)/[1/E_r - \{(1 - \nu_i^2)/E_i\}]$$

$$H_{IT} = \text{maximum load applied (in mN)}/\text{projected area (in nm}^2\text{)},$$

where, ν_s and ν_i are the Poisson ratio of the sample and that of the diamond indenter, respectively. E_r and E_i are the reduced modulus (combined modulus of indenter and sample) and elastic modulus of the indenter, respectively. The known value of the elastic modulus and Poisson ratio of the indenter are 1 141 GPa and 0.07, respectively. The

Table 1 Summary of the composition of the solution, probable formulation and the corresponding band gap energy of the films.

Amount of ions taken in the working solution (0.1 M)				Formulation of the films (as obtained from EDX)	Band gap (eV)
Bath	Pb^{2+} ion (ml)	Cd^{2+} ion (ml)	SeO_3^{2-} ion (ml)		
A	10	3	10	$Pb_{0.8}Cd_{0.2}Se$	0.9
B	10	5	10	$Pb_{0.7}Cd_{0.3}Se$	1.4
C	10	8	10	$Pb_{0.2}Cd_{0.8}Se$	1.7

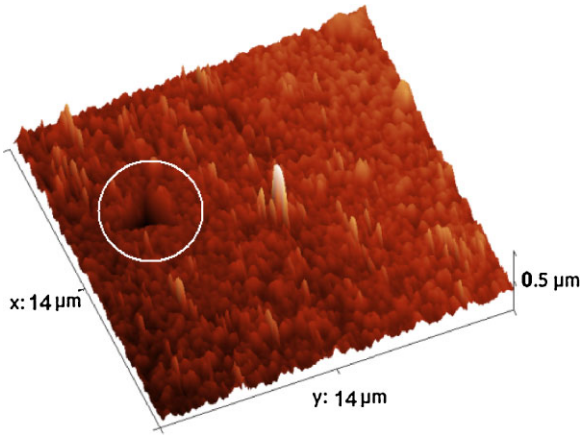

Figure 4 (online colour at: www.pss-a.com) AFM image of the thin film showing the impression of the diamond indenter on the film (within the white circle) which occurred during the nano-indentation measurement at 40 mN load.

nanoindentation characteristics at three different loads (using Berkovich indenter tip) of 20, 30 and 40 mN for the films grown from Bath A are shown in Fig. 5(a)–(c), for Bath B in Fig. 6 (a)–(c) and for Bath C in the Fig. 7 (a)–(c), respectively. From these figures it is evident that the maximum depth of penetration obtained in the coating surface is around 400 nm. The curves follow almost the same trend, which reveals that the localized mechanical properties of the films obtained from different baths have slight differences.

For the industrial applications of these films in the form of electronic devices like solar cells, laser diodes etc. there is a chance of such films being exposed to higher temperatures. At room temperature also, the films must show good mechanical properties like adherence with the substrate, hardness etc. for successful use in devices. If there is a large difference between the values of co-efficient of thermal expansion (CTE) of the film and the bottom layer, thermal stresses would result due to unequal expansion and contraction. It would deform the surface and hence decreases the sustainability/stability of the coating. The hardness values, H_v and the instrumented elastic modulus values, E_{IT} (in GPa) are presented in the Tables 2a–c, which reveals that both the hardness and the modulus of the coated surface decrease significantly with increase in the applied load. The hardness and modulus values are quite higher, although the load was increased from 20 to 40 mN. The higher hardness and elastic modulus refers to better resistance towards the deformation of the surface under thermal stresses and good adherence of the deposited film with the bottom layer. Among the three types of films, the highest hardness and elastic modulus (under three different loads) were shown by the films obtained from Bath A, whereas, the lowest values were shown by the films obtained from Bath B. Films from Baths C were found to show values in between the other two compositions. Though the films from Bath B ($Pb_{0.7}Cd_{0.3}Se$) show the lowest values of hardness and elastic modulus at different loads among the films from other two baths, it is sufficient enough to be used for their practical applications.

3.8 Electrical measurements DC *I–V* measurement of the SnO_2:F (TCO)/$Pb_{0.7}Cd_{0.3}Se$ hetero-structure

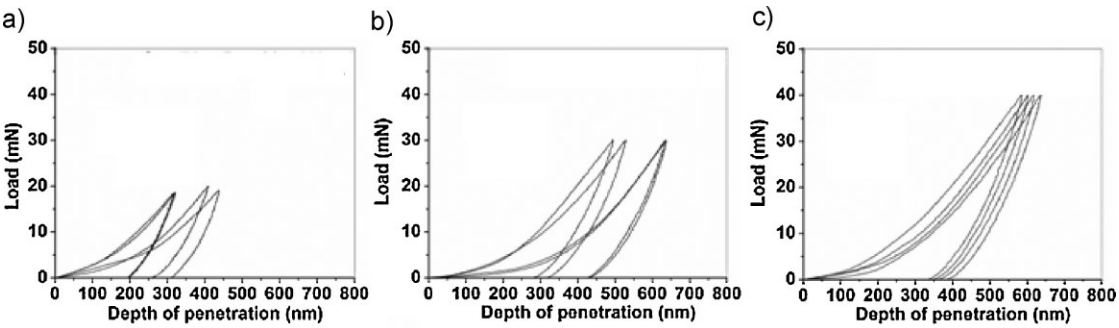

Figure 5 Load vs. depth of penetration plots at three different loads of (a) 20 mN, (b) 30 Mn, and (c) 40 mN for the films deposited from Bath A.

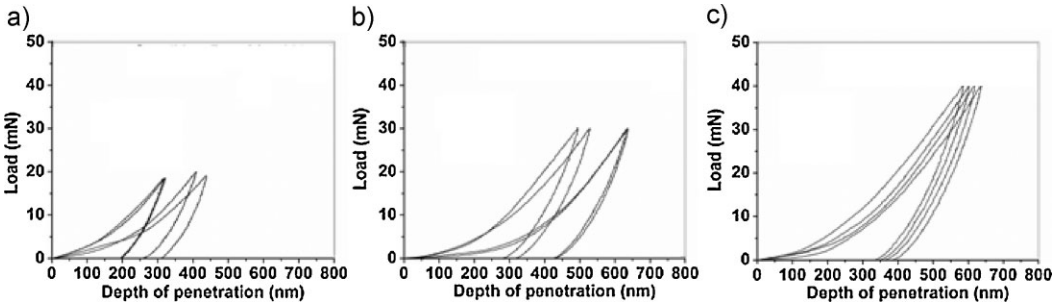

Figure 6 Load vs. depth of penetration plots at three different loads of (a) 20 mN, (b) 30 mN, and (c) 40 mN for the films deposited from Bath B.

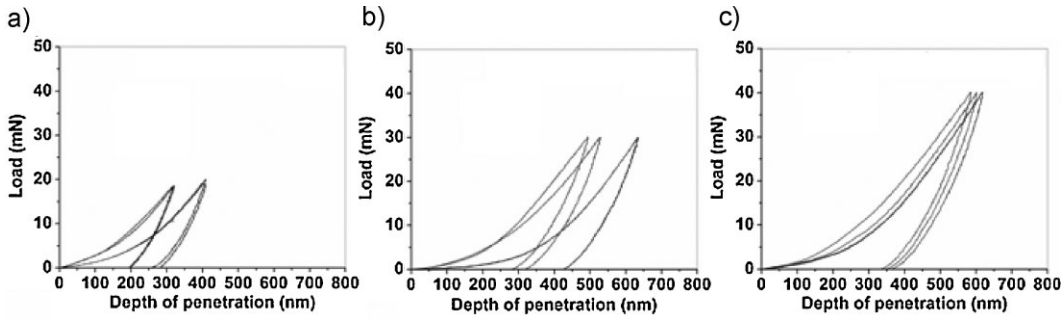

Figure 7 Load vs. depth of penetration plots at three different loads of (a) 20 mN, (b) 30 mN, and (c) 40 mN for the films deposited from Bath C.

Table 2a Hardness and elastic modulus at three different loads of Bath A.

Load (mN)	Hardness: H_v (Vickers)	Hardness: E_{IT} (GPa)	Modulus: E_{IT} (GPa)
20	858.44	9.120	143.05
30	706.21	6.970	109.80
40	615.26	6.521	99.51

Table 2b Hardness and elastic modulus at three different loads of Bath B.

Load (mN)	Hardness: H_v (Vickers)	Hardness: E_{IT} (GPa)	Modulus: E_{IT} (GPa)
20	768.84	8.302	132.03
30	686.19	6.471	100.60
40	599.22	6.210	91.21

Table 2c Hardness and elastic modulus at three different loads of Bath C.

Load (mN)	Hardness: H_v (Vickers)	Hardness: E_{IT} (GPa)	Modulus: E_{IT} (GPa)
20	801.47	8.521	139.07
30	715.11	6.671	108.30
40	625.65	6.381	94.71

was carried out in a voltage range of –1.0 to + 1.0 V and is shown in Fig. 8. The upper electrical contact to the film was made with colloidal Ag-paste with 0.09 cm^2 area, while, TCO itself acted as the bottom contact. From the rectifying nature of the *I–V* plot, it can be proposed that the deposited $Pb_{0.7}Cd_{0.3}Se$ film is p-type in nature. The threshold voltage of this p–n junction is about + 0.5 V, whereas, the onset of Zener effect occurs nearly at –0.5 V. From this plot, the DC resistance (r_{dc}) which is generally calculated at the point of

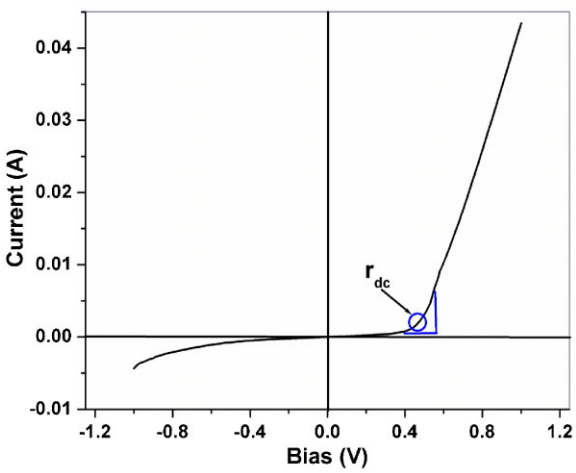

Figure 8 (online colour at: www.pss-a.com) DC *I–V* characteristic plot for SnO_2:F (TCO)/ $Pb_xCd_{1-x}Se$ hetero-structure.

threshold voltage, was found to be nearly 300 Ω, whereas, the AC resistance, $[\delta V/\delta I]r_{dc}$ was 0.033 Ω. The resistivity value at r_{dc} was calculated to be 6.75×10^5 Ω-cm.

4 Conclusion A simple galvanic technique has been developed to deposit ternary thin films of $Pb_xCd_{1-x}Se$ on TCO coated glass substrates, which involved no use of external energy. The deposition was found to be pH sensitive. The band gap energy for such films was found to be about 1.4 eV, which is close to ideal for the application as photovoltaic material. Films showed compact and dense surface morphology with cubic crystallites. The mechanical properties in terms of hardness and elastic modulus in case of films from Bath B are lowest among the three cases, but high enough for thin films, which is an indication for its good adhesiveness with the bottom substrate. Formation of a p–n junction with n-type TCO establishes the p-type conduction nature of the deposited $Pb_{0.7}Cd_{0.3}Se$ films.

Acknowledgements The authors N. Mukherjee, G. G. Khan and A. Sinha are thankful to CSIR, India for financial assistance (grant no. 8/3(0051)/2008-EMR-I, 8/3(0052)/2008-EMR-I and 8/3(0057)/2008-EMR-I, respectively). The authors are also thankful to Mr. Debashis Ghosh (M.Sc. final year student of the Dept. of Chemistry of this university) for his technical support.

References

[1] N. Bouad, M. C. Record, J. C. Tedenac, and R. M. Marin-Ayral, J. Solid State Chem. **177**, 221 (2004).
[2] H. K. Sachar, I. Chao, P. J. McCann, and X. M. Fang, J. Appl. Phys. **85**, 7398 (1999).
[3] C. Freed and J. W. Bielinski, Appl. Phys. Lett. **43**, 629 (1983).
[4] B. Sumpf, D. Göring, R. Haseloff, H. Ka, and J. W. Tomm, Collect. Czech. Chem. Commun. **54**, 284 (1989).
[5] J. M. Tomm, B. Sumpf, H. Ka, and A. Szczerbakow, Cryst. Res. Technol. **22**, 981 (1987).
[6] A. K. Sood, K. Wu, and J. N. Zemel, Thin Solid Films **48**, 73 (1978).
[7] N. Bouad, R. M. Marin-Aryal, and J. C. Tedenac, J. Alloys Compd. **297**, 312 (2000).
[8] P. P. Hankare, S. D. Delekar, P. A. Chate, S. D. Sabane, K. M. Garadkar, and V. M. Bhuse, Semicond. Sci. Technol. **20**, 257 (2005).
[9] E. A. Turner, H. Rösner, Y. Huang, and J. F. Corrigan, J. Phys. Chem. C **111**, 7319 (2007).
[10] N. Mukherjee, Sk. F. Ahmed, D. Mukherjee, K. K. Chattopadhyay, and A. Mondal, Phys. Status Solidi C **5**, 3458 (2008).
[11] K. R. Murali, I. Radhakrishna, K. N. Rao, and V. K. Venkatesan, J. Mater. Sci. **25**, 3521 (1990).
[12] J. J. Loferski, J. Appl. Phys. **27**, 777 (1956).
[13] G. A. Shaw, D. S. Stone, A. D. Johnson, A. B. Ellis, and W. C. Crone, Appl. Phys. Lett. **83**, 257 (2003).
[14] W. C. Oliver and G. M. Pharr, J. Mater. Res. **7**, 1564 (1992).

